New Journal of Physics
The open-access journal for physics

Effect of quantum confinement of surface electrons on adatom–adatom interactions

V S Stepanyuk[1], N N Negulyaev[2], L Niebergall[1] and P Bruno[1]

[1] Max-Planck-Institut für Mikrostrukturphysik, Weinberg 2, D-06120 Halle, Germany

[2] Fachbereich Physik, Martin-Luther-Universität, Halle-Wittenberg, Friedemann-Bach-Platz 6, D-06099 Halle, Germany

E-mail: stepanyu@mpi-halle.de

New Journal of Physics **9** (2007) 388

Received 25 June 2007

Published 31 October 2007

Online at http://www.njp.org/

doi:10.1088/1367-2630/9/10/388

Abstract. The quantum confinement of surface-state electrons in atomic-scale nanostructures is studied by means of the Korringa–Kohn–Rostoker (KKR) Green's function method. We demonstrate that the surface-state mediated interaction between adatoms can be significantly modified by the quantum confinement of surface electrons. We show that quantum corrals and quantum mirrors constructed on metal surfaces can be used to tailor the exchange interaction between magnetic adatoms at large distances. We discuss the self-organization of adatoms on metal surfaces caused by quantum confinement.

Contents

PII: S1367-2630(07)53550-0

1. Introduction

Surface-state electrons on the (111) surfaces of noble metals form a two-dimensional (2D) nearly free electron gas [1]. Such states are confined in a narrow layer at the surface. An electron in such a state *runs* along the surface, much like a 2D plane wave. The scattering of the surface electrons by adatoms leads to quantum-interference patterns in the local density of states (LDOS) and to the long-range (Friedel-type) oscillatory interaction between adsorbates [1]. The scanning tunneling microscope (STM) has enabled direct imaging in the real space of the quantum interference of surface electrons near adsorbates [2]–[4], steps [5]–[9] and on islands [10].

The indirect atomic interactions were first realized 50 years ago by Koutecky [11] and investigated theoretically by Grimley [12], Einstein and Schrieffer [13] and Lau and Kohn [14]. The first experimental evidence of the long-range oscillatory interaction (LRI) between adatoms was reported by Tsong [15]. Only recently, low-temperature STM studies have resolved long-range adsorbate interactions mediated by surface states at large interatomic separations [16, 17]. It has been shown that such interactions depend on the type of the adsorbate and the substrate. On surfaces supporting the surface-state electrons the LRI decays as $1/r^2$, where r is the interatomic distance, and oscillates with a period of $\lambda_F/2$ (λ_F is a surface state Fermi wavelength) [1]. For large adsorbate–adsorbate separations Hyldgaard and Persson [18] have found that the LRI can be described as the following:

$$E(r) = A_0 E_0 \left(\frac{2\sin\delta_0}{\pi}\right)^2 \frac{\sin(2k_F r + 2\delta_0)}{(k_F r)^2}. \tag{1}$$

Here, k_F is the Fermi surface wavevector, E_0 is the surface state band edge relative to the Fermi energy, δ_0 is the phase shift and A_0 is the scattering amplitude[3].

The equation (1) has been obtained through an asymptotic evaluation of the one-electron contributions to the interaction energy. Our *ab initio* calculations [19] have shown that in the case of Cu(111), the asymptotic equation (1) is accurate even down to a distance of $\lambda_F/2 \approx 15$ Å. The LRI between Co adatoms on Cu(111) determined experimentally and calculated by means of the Korringa–Kohn–Rostoker (KKR) Greens function method [19] is shown in figure 1. One can see that the agreement between the calculation and the experiment is very good.

The LRI can significantly affect the growth morphology at low temperatures [19]–[21]. Knorr *et al* [17] have proposed to exploit the surface-state mediated interactions between adatoms for the self-organization of long period ordered nanostructures. Recently, Silly *et al* [22, 23] have created a large ordered superlattice of Ce adatoms on Ag(111) exploiting the LRI. The kinetic Monte Carlo (kMC) simulations of Negulyaev *et al* [24, 25] have given clear evidence that the surface-state mediated long-range interaction between Ce adatoms on Ag(111) can lead to their self-assembly into linear chains and superlattices. The interatomic separation

[3] The variation in the LDOS (ΔLDOS) at the Fermi level originating from the interference of incident and scattered surface-state electrons at adatom sites is given by the formula:

$$\Delta\mathrm{LDOS}(r) \sim \frac{1}{k_F r}\left(\cos^2\left(k_F r - \frac{\pi}{4} + \delta_0\right) - \cos^2\left(k_F r - \frac{\pi}{4}\right)\right),$$

where δ_0 is the scattering phase shift, $k_F = \sqrt{2m_e E_0/\hbar^2}$ is the Fermi surface wavevector, E_0 is the surface-state band edge, m_e is the effective electron mass and r is the distance from the position of the center of an adatom [6].

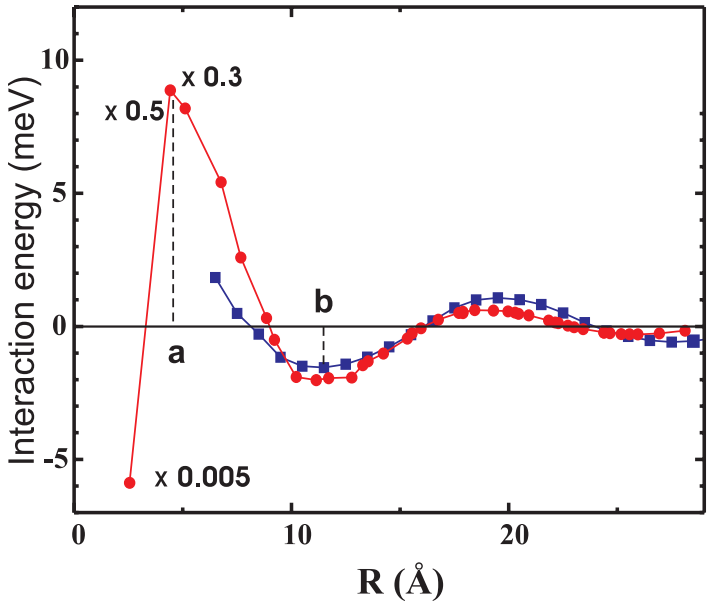

Figure 1. Experimental (blue) and theoretically calculated (red) interaction energies between two Co adatoms on Cu(111) [19].

in such structures has been found to correspond to the first minimum of the LRI potential. For example, on Cu(111) and Ag(111) this minimum is found to be at about 12 and 30 Å, respectively [1, 24, 25]. Adatom bonding in such nanostructures is determined by a long-range interaction between adatoms. In figure 2, we present results of the kMC for Ce superlattice on Ag(111) [24, 25].

Similar studies of Rogowska and Maciejewski [26] have shown that the surface-state mediated interactions between Cu adatoms lead to the formation of dilute nanostructures with an average nearest-neighbor distance a few times longer than an equilibrium adatom–adatom distance.

Surface-state electrons can also play an important role in magnetic interactions on metal surfaces. For example, it has been shown that the exchange interaction between magnetic adatoms at large distances is mediated by surface-state electrons [27].

Particularly, fascinating phenomena occur if the surface electrons are confined to closed structures such as quantum corrals, adislands or vacancy islands. The first observation of standing-wave patterns in the Fe corral on Cu(111) was reported by Crommie *et al* more than a decade ago [3]. Quantum confinement of surface electrons has been found on nanoislands [10] and in vacancy islands [28]. As an example we show in figure 3 the standing-wave patterns inside the Co corral on Cu(111) obtained by means of the KKR Green's function method [29].

Recent *ab initio* calculations and experiments have revealed the spin-dependent quantum confinement of surface electrons on Co nanoislands on Cu(111) [31, 32]. Quantum confinement of surface states on magnetic nanoislands has been shown to lead to the spin-selective quantum interference. The spin-polarization (SP) can be locally and energetically modulated by engineering the shape and the size of the surface-deposited nanostructure. As an example, we present in figure 4 the SP of surface-state electrons on a triangular Co island on Cu(111). A strongly inhomogeneous distribution of the SP on the island is clearly seen. We have shown

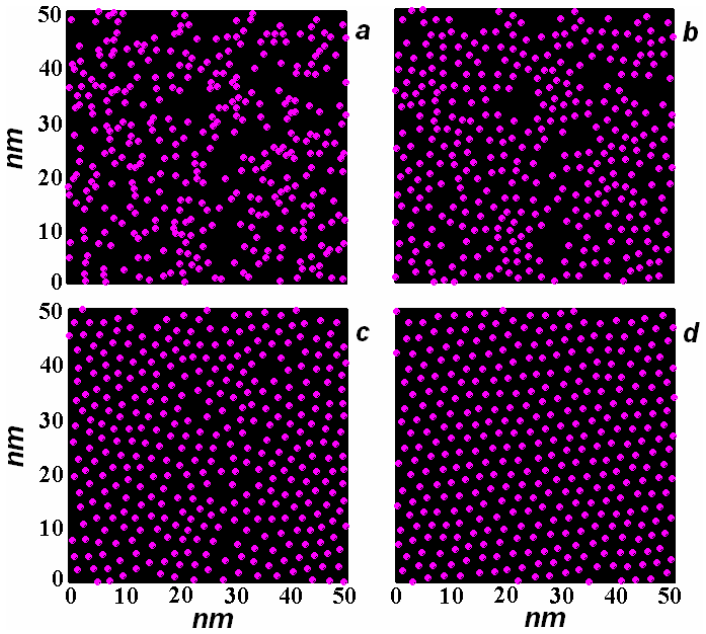

Figure 2. The kMC simulation of Ce adatoms on Ag(111). The concentration is 0.01 ML, temperature is 4.0 K. Pictures correspond to the following time intervals: (a) 0 s, (b) 0.4 s, (c) 3.9 s, (d) 240 s. In (d) the distance between nearest Ce atoms is close to 3 nm [24, 25].

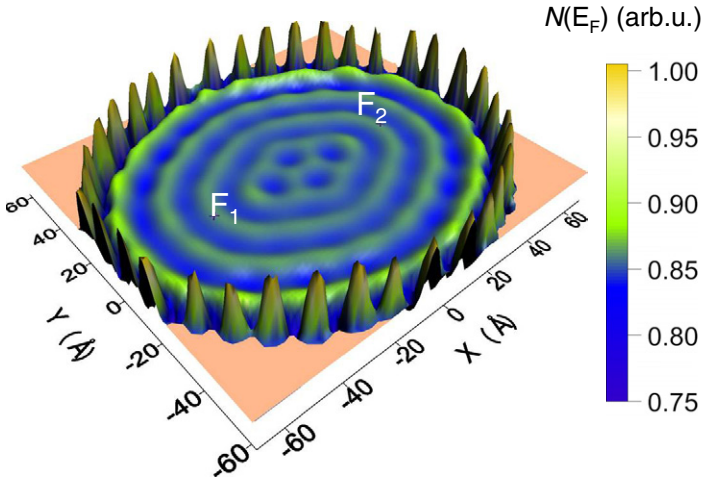

Figure 3. Standing-wave patterns inside the Co corral on Cu(111) [29]. The LDOS at the Fermi energy is shown. Geometrical parameters of the corral are the same as in the experimental setup of [30], i.e. semi-axis $a = 71.3$ Å and eccentricity $\varepsilon = 0.5$.

that a spatial variation of SP is exclusively caused by the quantum interference of the majority surface-state electrons. Our theoretical prediction has been confirmed by the experiment of Pietzsch *et al* [34].

Exploiting the quantum scattering of surface electrons in engineered nanostructures Manoharan *et al* [30] have discovered a novel method to transport information on the atomic

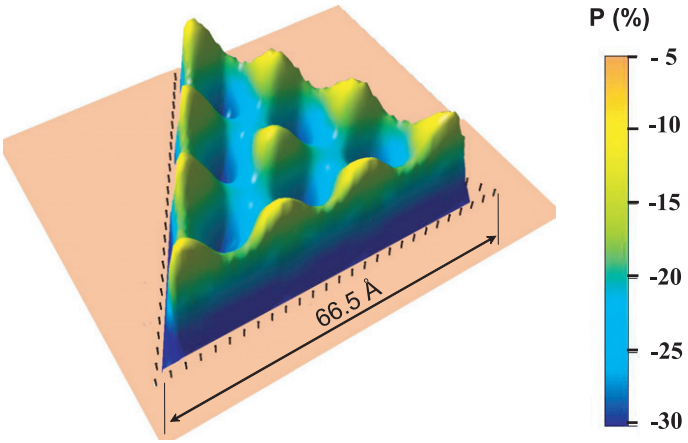

Figure 4. The spin-polarization of surface-state electrons on triangular Co island on Cu(111) [33]; calculations are performed for the energy $E = 0.5\,\text{eV}$ above the Fermi level.

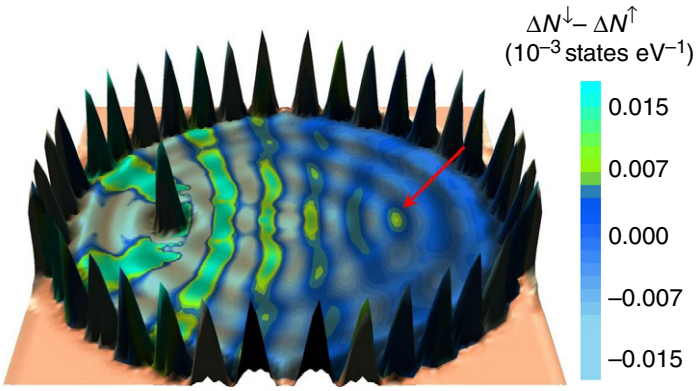

Figure 5. Quantum mirage. The LDOS at the Fermi energy on the Co adatom and the Co atoms of the corral walls are shown. The spin-polarization of surface-state electrons inside the Co corral is presented in color: $\Delta N^{\downarrow}$ and $\Delta N^{\uparrow}$ are determined by the difference between LDOS near the Fermi energy (+10 meV) of the Co corral with the Co adatom, the empty Co corral and the single Co adatom on the open Cu(111). The geometrical parameters of the corral are the following: semi-axis $a = 71.3\,\text{Å}$ and eccentricity $\varepsilon = 0.5$ [35].

scale. They have shown that the electronic structure of adatoms can be projected to a remote location using the quantum confinement of electronic states in corrals. Placing an atom of magnetic cobalt at one focus of the elliptical corral (constructed from several dozen cobalt atoms on Cu(111)) caused the Kondo effect to appear at the empty focus. In other words, they projected information about one atom to another spot where there was no atom. This fundamentally new way of guiding information on surfaces was called a mirage or phantom effect. Our *ab initio* studies have revealed that the SP of the cobalt adatom is projected to an empty focus (figure 5) [35].

Very recently, a novel phenomenon of the atomic self-organization caused by the quantum confinement has been predicted. *Ab initio* calculations and the kMC simulations have shown

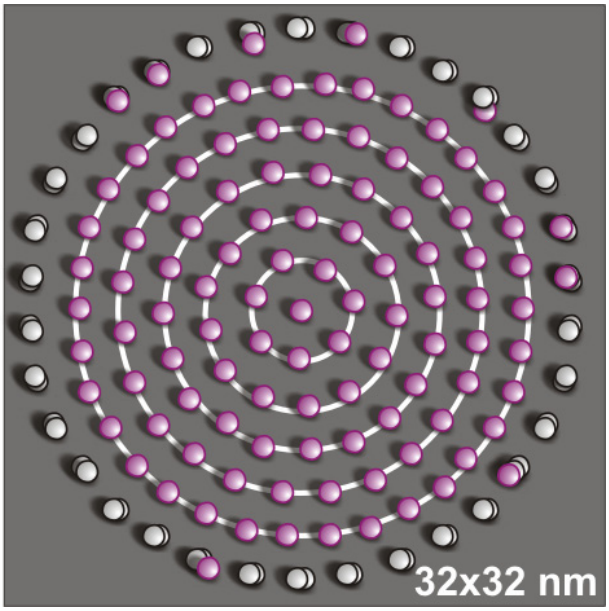

Figure 6. 'Quantum onion': self-assembly of Ce adatoms inside the Ce corral (semi-axis $a = 150$ Å, eccentricity $\varepsilon = 0$) made of Ce dimers on Ag(111). Temperature of the system is 4 K, Ce adatom coverage is 0.01 ML, Ce adatoms were deposited simultaneously [29].

that electronic states in quantum corrals can significantly modify the diffusion of adatoms at low temperatures and can lead to the self-organization of adatoms [29]. Self-organization of Ce adatoms inside the Ce corral into different concentric circular orbits, forming a structure which we call a 'quantum onion' is presented in figure 6.

In this paper, performing *ab initio* calculations, we demonstrate the effect of the quantum confinement of surface electrons on the long-range interaction between magnetic adatoms and their exchange coupling. The self-organization of adatoms due to quantum confinement is discussed.

2. *Ab initio* approach

We consider quantum corrals, vacancy islands and adislands on the same footing using the KKR Green's function method [28, 29, 33, 35, 36]. The basic idea of the KKR Green's function method is a hierarchical scheme for the construction of the Green's function of nanostructures on a metal surface by means of successive applications of Dyson's equation. We treat the surface as the 2D perturbation of the bulk. For the calculation of the ideal surface the nuclear charges of several monolayers are removed, thus creating two half crystals being practically uncoupled. Taking into account the 2D periodicity of the ideal surface, we find the structural Green's function by solving a Dyson equation self-consistently:

$$G_{LL'}^{jj'}(\mathbf{k}_\parallel, E) = \mathring{G}_{LL'}^{jj'}(\mathbf{k}_\parallel, E) + \sum_{j''L''} \mathring{G}_{LL''}^{jj''}(\mathbf{k}_\parallel, E)\Delta t_{L''}^{j''}(E) G_{L''L'}^{j''j'}(\mathbf{k}_\parallel, E). \tag{2}$$

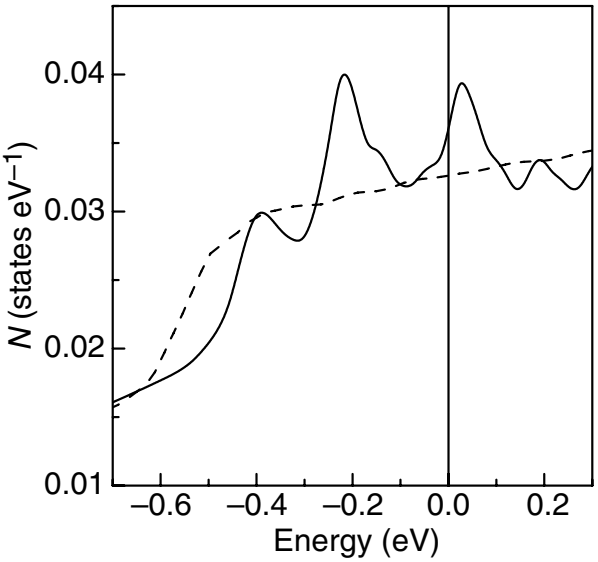

Figure 7. The LDOS at the corral focus. The elliptical Cu corral with semi-axis $a = 25\,\text{Å}$ and eccentricity $\varepsilon = 0.5$ on Cu(111) is considered. The LDOS of an open Cu(111) surface is shown by the dashed line [35].

Here, $\mathring{\mathrm{G}}$ is the structural Green's function of the bulk in a $\mathbf{k}_\parallel$-layer representation (j, j'-layer indices). The $\mathbf{k}_\parallel$ wavevector belongs to the 2D Brillouin zone, $\Delta t_L^j(E)$ is the perturbation of the t matrix to angular momentum $L = (l, m)$ in the jth layer. The consideration of corrals, vacancy islands or adislands on the surface destroys the translation symmetry. Therefore, the Green's function of such systems (quantum resonators) is calculated in a real space formulation. The structural Green's function of the ideal surface in real space representation is then used as the reference Green's function for the calculation of the quantum resonators from an algebraic Dyson equation:

$$G_{LL'}^{nn'}(E) = \mathring{\mathrm{G}}_{LL'}^{nn'}(E) + \sum_{n''L''} \mathring{\mathrm{G}}_{LL''}^{nn''}(E)\Delta t_{L''}^{n''}(E) G_{L''L'}^{n''n'}(E), \tag{3}$$

where $G_{LL'}^{nn'}(E)$ is the energy-dependent structural Green's function matrix and $\mathring{\mathrm{G}}_{LL''}^{nn''}(E)$ the corresponding matrix for the ideal surface, serving as a reference system, $\Delta t_L^n(E)$ describes the difference in the scattering properties at site n induced by the existence of the adsorbate atom. Multiple scattering of surface-state electrons inside the resonators (including the interaction with bulk states) is taken into account in our approach. Our studies have proved that only a limited number of atoms near the resonator walls contribute to $\Delta t_L^n(E)$ in equation (3). Therefore, even very large resonators can be calculated fully *ab initio* using our approach [28, 33, 35].

3. Results and discussion

3.1. Adatom–adatom interactions

The behavior of surface-state electrons in quantum resonators is determined by the quantum interference between the electron waves traveling towards edges of the resonator and the

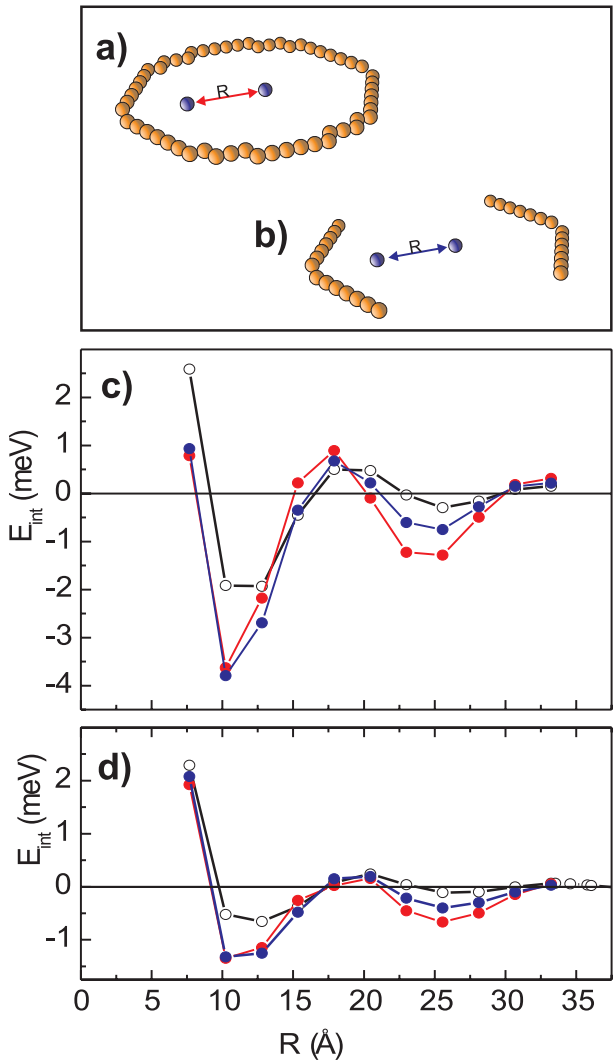

Figure 8. (a) The elliptical corral with semi-axis $a = 25$ Å, and eccentricity $\varepsilon = 0.5$ is considered. The first Co (Cr) adatom is placed at one focus. (b) A quantum 'mirror' is made by removing several atoms of the corral. The energy interaction between two Co (c) and two Cr (d) adatoms placed inside the Cu corral (red), between 'mirrors' (blue) and on open Cu(111) surface (black).

backscattered waves. In figure 7, we demonstrate the energy-resolved LDOS in the Cu corral. The LDOS is presented at the corral's focus. One can see that the corral significantly influences the LDOS. Resonant peaks of the LDOS indicate the quantum confinement. These results suggest that quantum corrals can be used to locally modify the density of electrons on a surface and can affect the energy of atoms placed inside the corral. On an open surface adatoms interact through the fact that the adsorbtion energy of one adatom depends on the electron density which oscillates around the other (the decay law is $1/r$ (see footnote 3)). Note, on an open surface adatoms are placed in a 2D electron gas with constant density of surface electrons (for example, on Cu(111) the surface state has an occupancy of about 1/25 of an electron per surface unit cell). However, if surface electrons are confined, the density of electronic states exhibits a strongly

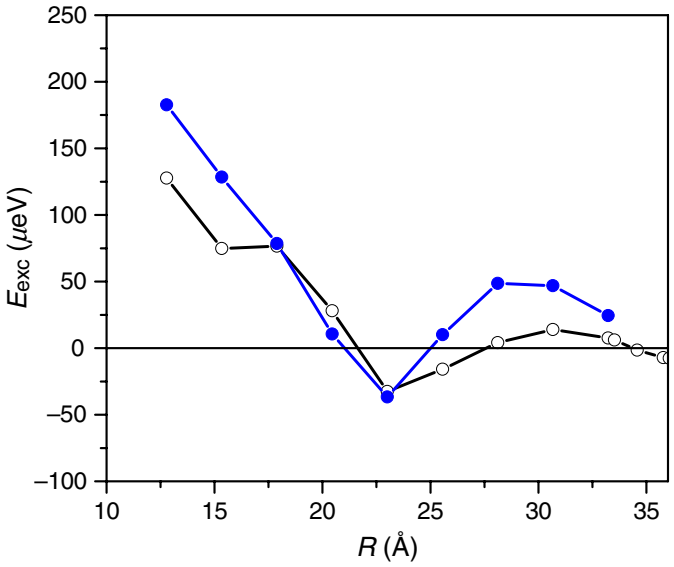

Figure 9. The exchange interaction between two Cr adatoms placed between two mirrors and on an open Cu(111) surface, see figure 8.

inhomogeneous spatial distribution, as shown in figure 3. Therefore, the surface-state mediated long-range interaction between adatoms can be affected by confined surface electrons. We have performed *ab initio* calculations for the interaction between two Cr adatoms and two Co adatoms on an open Cu(111) surface and inside Cu corrals on Cu(111). Results presented in figure 8 show that the quantum confinement of surface electrons significantly affects the interaction between adatoms. The surface-state mediated interaction between adatoms in corrals at large distances can be strongly enhanced compared to that on an open surface. The driving force behind this effect is related to the quantum confinement of surface electrons.

Note, the long-range interaction between Co adatoms is stronger than between Cr adatoms. Such difference could be explained by the fact that the wave functions of Cr are more extended and therefore, the scattering of surface electrons into the bulk at the Cr adatom is stronger than for the Co adatoms. The geometry of the resonator affects only the interaction strength, while leaving the modulation period essentially unchanged, since the Fermi wavevector does not depend on the geometry.

The interaction between adatoms can be tailored by designing quantum resonators of different shapes. For example, we create an 'open resonator' consisting of two semielliptical arrangements of Cu atoms (figure 8). Results shown in figure 8 clearly demonstrate that the quantum interference of surface electrons between these two 'mirrors' modifies the interaction between adatoms. Such quantum resonators can be also used to affect the indirect exchange interaction between adatoms. Figure 9 depicts the exchange interaction between Cr adatoms placed between 'mirrors' in comparison to that on an open Cu(111) surface. These results demonstrate that the quantum confinement can enhance the exchange interaction between magnetic adatoms at large separations. Recalling our recent results on the exchange interaction between adatoms in corrals of different eccentricities [35], one can conclude that it could be possible to modulate the magnetic interactions between adatoms at large distances by engineering the shape and the size of the quantum resonators.

3.2. The adatom self-organization

We investigate the self-assembly of adatoms on noble (111) metal surfaces in the presence of several quantum resonators. Randomly distributed circled quantum corrals have been used to model a surface with resonators. Such a situation corresponds, for example, to the system of vacancy islands or nanoislands on a surface. The walls of each corral are made of dimers. It is well known that the dimer has larger diffusion barrier than the monomer, that provides the temperature stability of the resonators. As a result, atomic self-assembly takes place, while the walls of the corral are immobile. Two particular systems are considered within our study: self-assembly of (i) Co adatoms at the presence of Co corrals on a Cu(111) surface and (ii) Ce adatoms at the presence of Ce corrals on a Ag(111) surface.

One may expect that adatoms on a surface interact not only electronically but also elastically [37]. However, our previous calculations [38] indicate that the elastic interactions are considerably weaker than electronic ones at interatomic separations >7 Å. Therefore, one can neglect the influence of elastic effects on an atomic self-assembly in the studied systems.

For our investigations we use the rejection-free kMC method of Fichthorn and Weinberg [39]. The (111) surface is represented as a triangular lattice of fcc and hcp hollow sites with the separation $r_0/\sqrt{3}$ between the nearest sites. The nearest neighbor (NN) distance for the Cu(111) surface r_0 is 2.56 Å and for the Ag(111) surface r_0 is 2.89 Å. The hop rate of an adatom from site k to site j on the (111) surface is calculated using the expression $v_{k\to j} = v_0 \exp(-E_{k\to j}/k_B T)$, where T is the temperature of the substrate, v_0 is the attempt frequency and k_B is the Boltzmann factor. We set v_0 to $10^{12}\,s^{-1}$. The influence of the LRI on adatom diffusion is included in the hopping barrier [20, 40, 41] which takes the form: $E_{k\to j} = E_D + 0.5(E_j - E_k)$. Here, E_D is the diffusion barrier for an isolated atom on a clean surface, $E_{k(j)}$ is the sum of the pair interactions of the hopping adatom with all other adatoms in the system (including the atoms of the corral walls), if the adatom is at site $k(j)$. According to the exploited algorithm three short jumps to the different neighboring positions can occur for each adatom on the (111) surface. If the number of adatoms in the system is equal to N, then $3N$ different hops with the rates $v_1, v_2, \ldots, v_{3N}$ are possible on every step of the kMC algorithm. The time interval between two steps can be calculated:

$$\tau = -\ln U \Big/ \sum_{i=1}^{3N} v_i, \tag{4}$$

where U is a randomly distributed number in the interval (0, 1). The magnitude of the diffusion barrier E_D for a single Co adatom on a Cu(111) surface equals to 37 meV [19]. The magnitude of E_D for a single Ce adatom diffusion on the Ag(111) is considered to be 9 meV according the experimental studies of the group of Schneider [22, 23]. In the framework of our kMC studies the interaction energy between Co adatoms on Cu(111) is determined by means of the KKR Green's function method (cf figure 1). The interaction between two Ce adatoms on Ag(111) surface is calculated using the model of Hyldgaard and Persson (equation (1)) where the parameters are taken from the experimental studies of Silly *et al* [22, 23]. We perform our simulations with the following values of the parameters: $A_0 = 0.30$, $\delta_0 = 0.42\pi$. Periodic boundary conditions on the surface are applied in our calculations. Adatoms are deposited on the (111) surface randomly and simultaneously. For the analysis of our results we exploit the

radial distribution function (RDF) $f(r)$:

$$f(r) = \frac{S}{4\pi r N^2} \left\langle \sum_{i=1}^{N} \sum_{j \neq i} \delta(r - r_{ij}) \right\rangle = \frac{\rho(r)}{\rho_0}, \tag{5}$$

where S is a square of the considered simulation cell, $\rho(r)$ and ρ_0 are local and equilibrium densities of deposited adatoms correspondingly. Usually this function is used for homogeneous and isotropic systems to characterize the structural correlations. Function $f(r)$ gives the probability to find an adatom at a distance r from an adatom placed at the origin of the coordinate system. Within our analysis the origin of the coordinate system is considered to coincide with the geometrical centers of the corrals. Peaks (maxima) in the RDF correspond to the positions (orbits) with high occupation probability, while minima correspond to the orbits with low occupation probability.

To create a macroscopic-ordered pattern of atoms exploiting the LRI one has to deposit adatoms with an optimal coverage ρ_0. The distance between nearest atoms in the pattern should correspond to the position of the local minimum b in LRI potential (cf figure 1). Therefore, one can estimate the magnitude of ρ_0 from the ratio $\rho_0 = (r_0/b)^2$ ML. For Co atoms on the Cu(111) surface $b = 1.1$ nm, hence the optimal coverage ρ_0 equals to 0.06 ML. For Ce atoms on the Ag(111) surface b is about 3.0 nm, therefore $\rho_0 = 0.01$ ML.

First, we discuss the results concerning the self-assembly of Co adatoms on the Cu(111) surface. The size of the simulation cell is 400×400 Å. The temperature of the system is 13 K, the coverage ρ_0 is about 0.06 ML. Five Co corrals are considered (the radii of each corral is 42 Å). The self-assembly of Co adatoms is well seen: adatoms tend to occupy positions only near the allowed orbits inside and outside the corral. Formation of four pronounced orbits inside each corral is well seen in figure 10. The distance between the nearest Co adatoms located on the same orbit is about 12 Å, corresponding to the position of the first local minimum in the LRI between two Co adatoms on the Cu(111) (cf figure 1). Dimer and trimer formation which occurs due to deposition processes and weak LRI prevent the formation of the nanostructure with the ideal circle orbits. Figure 11 demonstrates the RDF for the system of Co adatoms self-assembled on the Cu(111) in the presence of Co corrals (figure 10). The blue vertical line marks the border of the resonator (the position of the corral walls). The RDF has four pronounced peaks at $r < 42$ Å, which correspond to the orbits shown in figure 10. The first peak at $r = 4$ Å corresponds to the first orbit inside the resonator. The first minimum at $r = 8$ Å is related to the area between the first and the second orbits: the probability of finding a Co adatom in this region is low. The next peaks in the RDF (the second at 13 Å, the third at 23 Å and the fourth at 32 Å) correspond to the orbits with larger diameters. The amplitude of the peaks increases as we approach the corral walls. When r is close to 42 Å (the position of the corral walls) two small peaks can be resolved. These peaks correspond to Co adatoms attached to the resonator walls from the inner and outer sides during the deposition process. There are also oscillations in the RDF outside corrals. Amplitudes of the corresponding peaks outside the corral are smaller than inside. This indicates that the effect of the confinement inside the corral is more pronounced than outside.

Now we turn to the results concerning the self-assembly of Ce adatoms on a Ag(111) surface at the presence of Ce resonators. The size of the simulation cell is 1000×1000 Å. The temperature of the system is 4 K, the coverage ρ_0 is about 0.01 ML. Five Ce corrals are randomly distributed on Ag(111) (the radii of each corral equals 100 Å). The self-assembly of Ce adatoms is well seen in figure 12: adatoms tend to occupy positions only near the circled

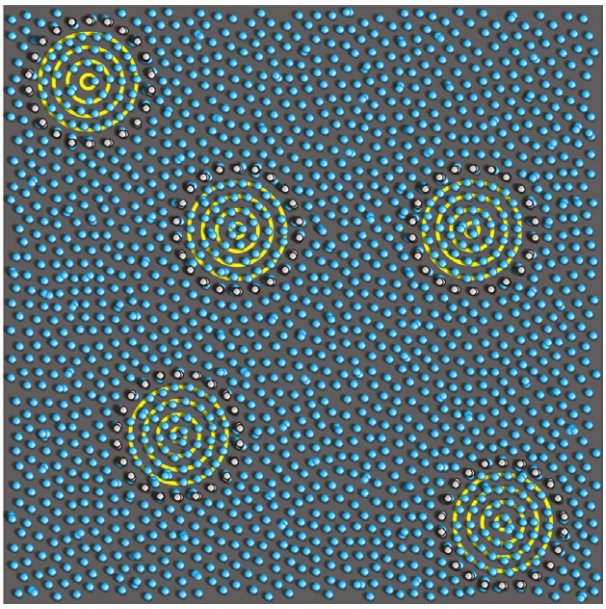

Figure 10. Self-assembly of Co adatoms on a Cu(111) surface in the presence of five Co corrals. Corrals are made from dimers. The distance between the Co dimers in corrals is about 12 Å. The radii of each corral is 42 Å. The temperature of the system is 13 K, the coverage of Co is 0.06 ML. The size of the area is 400×400 Å.

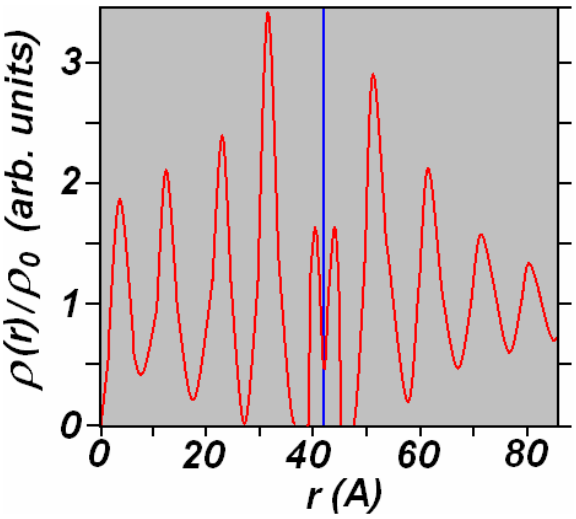

Figure 11. The RDF for Co adatoms on Cu(111) at a coverage of 0.06 ML at 13 K in the presence of corrals.

orbits inside and outside the corral. The existence of four orbits inside each corral is clearly seen. The distance between the nearest Ce adatoms is about 30 Å, which corresponds to the position of the first local minimum in the LRI between two Ce adatoms on Ag(111) [22]–[25]. The probability of the formation of Ce dimers during the deposition process is very small, because the coverage of deposited atoms is six times smaller than for Co on Cu(111). As a

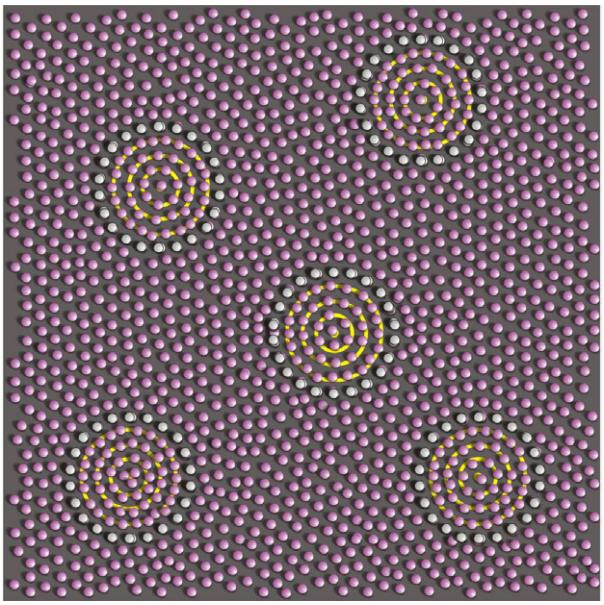

Figure 12. Self-assembly of Ce adatoms on a Ag(111) surface in the presence of five Ce corrals. Corrals are made from dimers. The distance between the Ce dimers in corrals is about 30 Å. The radii of each corral is 100 Å. The temperature of the system is 4 K, the coverage of Ce is 0.01 ML. The size of the area is 1000×1000 Å.

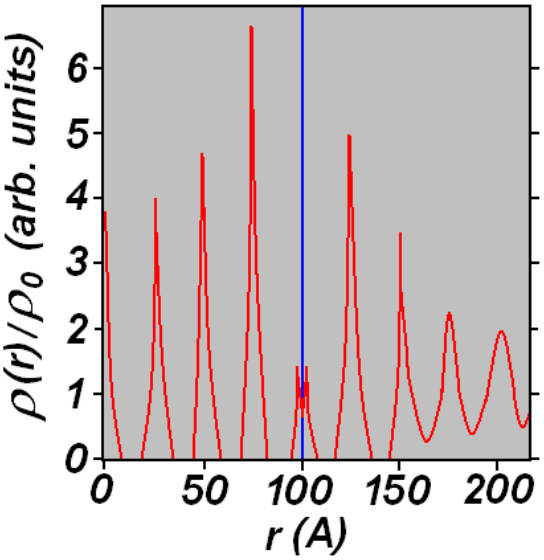

Figure 13. The RDF for Ce adatoms on Ag(111) at a coverage of 0.01 ML at 4 K in the presence of corrals.

result, Ce adatoms form a well ordered superstructure inside resonators. The RDF shown in figure 13 proves our findings. The blue vertical line marks the border of the resonators (corral walls). The RDF has four pronounced peaks inside the corral ($r < 100$ Å), which correspond to four different atomic orbits.

It is interesting to note that the difference between the self-organization of Co adatoms on Cu(111) and Ce adatoms on Ag(111) is determined by the formation of dimers during deposition. The concentration of dimers at the optimal coverage ρ_0 depends on the relative position of the first maximum a in the LRI potential and the first minimum b (cf figure 1), i.e. $\gamma = a/b$. A lower value of γ corresponds to a lower concentration of dimers. For Co atoms on the Cu(111) surface the magnitude of γ equals 0.45, and a significant number of immobile dimers preventing the self-assembly of randomly distributed atoms is formed. For Ce atoms on the Ag(111) surface the magnitude of γ is rather small (0.16), and only a few dimers are formed. As a result, the Ce atomic pattern exhibits a well-ordered structure.

4. Conclusion

Our findings have shown that the confinement of surface-state electrons in quantum resonators can affect the long-range interaction between adatoms. We have revealed that the quantum interference of surface-electrons inside corrals and between two 'quantum mirrors' modifies the interaction between magnetic adatoms and their magnetic coupling. It is possible to enhance the exchange interaction at large adatom–adatom separations exploiting the confinement of surface-electrons in artificial atomic nanostructures. Our work predicts that new magnetic nanostructures can be engineered at low temperatures exploiting the quantum confinement of surface electrons and surface-state mediated interactions.

Acknowledgment

This work was supported by Deutsche Forschungsgemeinschaft (DFG, SPP1165, SPP1153).

References

[1] Bürgi L, Knorr N, Brune H, Schneider M A and Kern K 2002 *Appl. Phys.* A **75** 141
[2] Brune H, Wintterlin J, Ertl G and Behm R J 1990 *Europhys. Lett.* **13** 123
[3] Crommie M F, Lutz C P and Eigler D M 1993 *Science* **262** 218
[4] Avouris Ph, Lyo I-W, Walkup R E and Hasegawa Y 1994 *J. Vac. Sci. Technol.* B **12** 1447
[5] Davis L C, Everson M P, Jaklevic R C and Shen W 1991 *Phys. Rev.* B **43** 3821
[6] Crommie M F, Lutz C P and Eigler D M 1993 *Nature* **363** 524
[7] Hasegawa Y and Avouris Ph 1993 *Phys. Rev. Lett.* **71** 1071
[8] Garsia J M, Sanchez O, Segovia P, Ortega J E, Alvarez J, Vazquez de Parga A L and Miranda R 1995 *Appl. Phys.* A **61** 609
[9] Petersen L, Laitenberger P, Lægsgaard E and Besenbacher F 1998 *Phys. Rev.* B **58** 7361
[10] Li J T, Schneider W-D, Berndt R, Bryant O R and Crampin S 1998 *Phys. Rev. Lett.* **81** 4464
[11] Koutecky J 1958 *Trans. Faraday Soc.* **54** 1038
[12] Grimley T B 1967 *Proc. Phys. Soc.* **90** 751
[13] Einstein T L and Schrieffer J R 1973 *Phys. Rev.* B **7** 3629
[14] Lau K H and Kohn W 1978 *Surf. Sci.* **75** 69

[15] Tsong T T 1973 *Phys. Rev. Lett.* **31** 1207
[16] Repp J, Moresco F, Meyer G, Rieder K-H, Hyldgaard P and Persson M 2000 *Phys. Rev. Lett.* **85** 2981
[17] Knorr N, Brune H, Epple M, Hirstein A, Schneider M A and Kern K 2002 *Phys. Rev.* B **65** 115420
[18] Hyldgaard P and Persson M 2000 *J. Phys.: Condens. Matter* **12** L13
[19] Stepanyuk V S, Baranov A N, Tsivlin D V, Hergert W, Bruno P, Knorr N, Schneider M A and Kern K 2003 *Phys. Rev.* B **68** 205410
[20] Fichthorn K A and Scheffler M 2000 *Phys. Rev. Lett.* **84** 5371
[21] Merrick M L, Luo W and Fichthorn K A 2003 *Prog. Surf. Sci.* **72** 117 and references therein
[22] Silly F, Pivetta M, Ternes M, Patthey F, Pelz J P and Schneider W-D 2004 *Phys. Rev. Lett.* **92** 016101
[23] Silly F, Pivetta M, Ternes M, Patthey F, Pelz J P and Schneider W-D 2004 *New J. Phys.* **6** 16
[24] Negulyaev N N, Stepanyuk V S, Hergert W, Fangohr H and Bruno P 2006 *Surf. Sci.* **600** L58
[25] Negulyaev N N, Stepanyuk V S, Niebergall L, Hergert W, Fangohr H and Bruno P 2006 *Phys. Rev.* B **74** 035421
[26] Rogowska J M and Maciejewski M 2006 *Phys. Rev.* B **74** 235402
[27] Stepanyuk V S, Niebergall L, Longo R C, Hergert W and Bruno P 2004 *Phys. Rev.* B **70** 075414
[28] Niebergall L, Rodary G, Ding H F, Sander D, Stepanyuk V S, Bruno P and Kirschner J 2006 *Phys. Rev.* B **74** 195436
[29] Stepanyuk V S, Negulyaev N N, Niebergall L, Longo R C and Bruno P 2006 *Phys. Rev. Lett.* **97** 186403
[30] Manoharan H C, Lutz C P and Eigler D M 2000 *Nature* **403** 512
[31] Diekhöner L, Schneider M A, Baranov A N, Stepanyuk V S, Bruno P and Kern K 2003 *Phys. Rev. Lett.* **90** 236801
[32] Pietzsch O, Kubetzka A, Bode M and Wiesendanger R 2004 *Phys. Rev. Lett.* **92** 057202
[33] Niebergall L, Stepanyuk V S, Berakdar J and Bruno P 2006 *Phys. Rev. Lett.* **96** 127204
[34] Pietzsch O, Okatov S, Kubetzka A, Bode M, Heinze S, Lichtenstein A and Wiesendanger R 2006 *Phys. Rev. Lett.* **96** 237203
[35] Stepanyuk V S, Niebergall L, Hergert W and Bruno P 2005 *Phys. Rev. Lett.* **94** 187201
[36] Wildberger K, Stepanyuk V S, Lang P, Zeller R and Dederichs P H 1995 *Phys. Rev. Lett.* **75** 509
[37] Lau K H and Kohn W 1977 *Surf. Sci.* **65** 607
[38] Longo R C, Stepanyuk V S and Kirschner J 2006 *J. Phys.: Condens. Matter* **18** 9143
[39] Fichthorn K A and Weinberg W H 1991 *J. Chem. Phys.* **95** 1090
[40] Ovesson S, Bogicevic A, Wahnström G and Lundqvist B 2001 *Phys. Rev.* B **64** 125423
[41] Fichthorn K A, Merrick M L and Scheffler M 2003 *Phys. Rev.* B **68** 041404